

**Fano resonance scattering in waveguide with an impedance
boundary condition**

Lei Xiong^{a)}, Wenping Bi, and Yves Aurégan

Laboratoire d'Acoustique de l'Université du Maine

UMR CNRS 6613,

Avenue Olivier Messiaen, 72085 Le Mans Cedex 9, France

August 19, 2018

^{a)}lei.xiong@univ-lemans.fr

Abstract

Sound propagation in a waveguide lined with one section of locally reactive material is studied by resonance scattering approach. The objective is to understand the effects of mode coupling in the lined section on the transmission. It is shown that a transmission zero is present in the vicinity of a resonance peak when a numerically real resonance frequency of the *open* lined section (opened to infinities through the rigid parts of the waveguide) is crossed. The transmission zero and immediate resonance peak form a Fano resonance, it has been explained as an interaction between a resonance and the non-resonant background. The real resonance frequency and its corresponding trapped mode are formed by the interferences (couplings) between two neighbor modes with complex resonance frequencies. It is also linked to the avoided crossing of eigenvalues and the exceptional point. The scattering matrix is expressed in terms of a matrix \mathbf{H}_{eff} which describes approximately the complex resonances in the *open* lined section. With the aid of the eigenvalues and eigenfunctions of matrix \mathbf{H}_{eff} , the traditional acoustic resonance scattering formula can be extended to describe the coupling effects between the *open* lined section and the rigid parts of the waveguide.

PACS Numbers: 43.20.Mv, 43.20.Ks

I. INTRODUCTION

Acoustic liners are commonly used in noise control devices for duct systems. Typical applications include silencers for ventilation systems, wall treatments for aircraft engines, and silencers for industrial gas turbines. To increase the liner efficiency, various strategies can be used. One is to find a new material design for which the impedance is close to the optimal value in the targeted range of frequencies^{1,2}. Another strategy is to take advantage of the acoustic impedance changes (like discontinuities) in axial^{3,4,5} or circumferential^{6,7} segments, or both of them^{8,9}. The strategy used in this paper is different: The idea is to couple the incoming propagative mode in the waveguide with the modes localized in the lined region. Those localized modes exist for particular values of the geometry in a uniform liner but can also be created by impedance variations. As an example, a very simple 2D model with an uniform liner is analyzed in this paper.

Such interferences between resonances and scattering appear in Fano resonances (for review articles see, for example, Refs. 10 and 11, and the references therein). In contrast to the conventional isolated resonances scattering, Fano resonance is explained by constructive and destructive interferences between a resonance (trapped mode) or a complex resonance (quasi-trapped mode) and the background or nonresonant scattering¹². A transmission zero is produced as a real resonance frequency is crossed¹³.

One of the crucial ingredients to form a Fano resonance is to have trapped mode with a real resonance frequency. Trapped modes are localized

oscillations in unbounded media and do not radiate energy to infinity. They were first observed experimentally in acoustics by Parker in 1966¹⁴. Discrete trapped modes may exist below the first cut-off frequency of the transverse modes, provided that some kinds of defect or variations of geometry exist^{15,16}. Discrete trapped modes may also exist above the first cut-off frequency for specific parameter combinations, they are called embedded trapped modes¹⁵ or bound states in continuum (BIC) in quantum mechanics¹⁷. Friedrich and Wintgen¹⁸ demonstrated that BIC is a natural feature of common physical situations, and can occur due to the interference of resonances. They have linked BICs directly to the phenomenon of an avoided crossing of neighbored resonance states (modes with complex eigenvalues). Recently, BICs in the vicinity of exceptional points were also found in open quantum billiards¹⁹. Sadreev *et al.*¹⁹ found that the BICs are close to the points of degeneracy of the closed quantum system. When the system is opened, the degeneracies are lifted and avoided crossings occur.

Fano resonance scatterings in acoustics and their relations with trapped modes in waveguides including obstacles or in duct-cavity systems have been studied by Hein *et al.*^{20,13}. They used finite-element method to compute numerically the acoustic resonances as well as transmission and reflection for an incoming duct mode. They obtained complex resonance frequencies and corresponding eigenfunctions, the homogeneous solutions of the Helmholtz equation with absorbing boundary conditions. The complex resonance frequencies are the positions of the poles of scattering matrix of the corresponding scat-

tering problem. Fano resonance scatterings were related to three types of trapped modes: antisymmetric (about duct axis) trapped modes below the first cut-off frequency, embedded trapped modes linked to avoided crossings of resonances, and trapped modes associated with Fabry-Pérot interferences between cavities.

In this paper, we study sound propagation in a waveguide lined on a section with a locally reacting material by the resonance scattering approach²¹. The objective is to understand the effects of mode coupling on the transmission of the lined section. We show that by varying a control parameter (the section length or the product of the lined admittance and the frequency), two neighbored modes with complex resonance frequencies interfere in the scattering region: the lined section opened to the two semi-infinite waveguides. In the vicinity of an exceptional point, where the eigenvalues and eigenfunctions coalesce, one mode turns to be trapped, the corresponding resonance frequency (eigenvalue) is real. A transmission zero is present in the vicinity of a resonance peak when the real resonance frequency is crossed, this is also called Fano resonance (section III).

In section II, we derive the Scattering matrix (S matrix). For that, we project the Helmholtz equation over the eigenfunctions of the rigid closed counterpart of the *open* lined section which form an orthogonal and complete function basis. The used eigenfunctions include the transverse and axial components, thus this method generalizes the Multimodal method⁹ in which the wave function is expanded only in terms of transverse eigenfunctions.

We express the scattering matrix S in terms of an effective matrix H_{eff} . The matrix H_{eff} approximately describes the complex resonances of the *open* lined section. Its eigenvalues are complex and give the poles of the S matrix. With the help of its eigenfunctions, we can extend the traditional acoustic resonance scattering formula²¹ to describe the coupling effects between the *open* lined section and the rigid waveguide.

II. MODEL

We consider the acoustic scattering problem in a two-dimensional infinite waveguide lined over a finite length a with a locally reacting material, as shown in Fig. 1. The waveguide is decomposed into three parts: two semi-infinite rigid waveguides $x \leq 0$ and $x \geq a$ (regions I and III, respectively), and one scattering region (region II). Time dependence is assumed as $\exp(-j\omega t)$ and will be omitted in the following. In the following, all the quantities are non-dimensionalized. The sound pressure $p(x, y)$ in the waveguide satisfies the non-dimensional Helmholtz equation

$$\left(\frac{\partial^2}{\partial x^2} + \frac{\partial^2}{\partial y^2} + K^2 \right) p(x, y) = 0, \quad (1)$$

where $K = (\omega/c_0)h$ refers to dimensionless frequency, ω is the frequency, c_0 is the sound velocity, and h is the height of the waveguide. Sound pressure p and coordinates (x and y) are normalized by $\rho_0 c_0^2$ and h , respectively, with ρ_0 the air density. The transverse boundary conditions in regions I, III, and

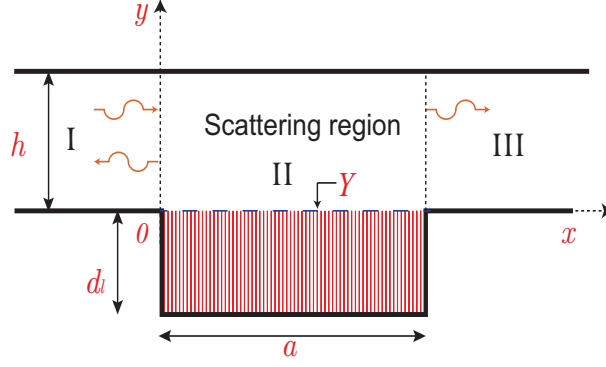


Figure 1: (Color online) A two-dimensional infinite waveguide lined with a locally reacting material of length a . Y refers to the admittance. The closed counterpart of the scattering region is called *closed cavity*, with rigid conditions at $x = 0$ and $x = a$.

II are

$$\left. \frac{\partial p}{\partial y} \right|_{y=0 \text{ and } 1} = 0 \text{ (for regions I and III)} \quad (2)$$

and

$$\left. \frac{\partial p}{\partial y} \right|_{y=0} = -jKYp \text{ and } \left. \frac{\partial p}{\partial y} \right|_{y=1} = 0 \text{ (for region II),} \quad (3)$$

respectively.

Inspired by the R-matrix method^{22,23}, the sound pressure $p(x, y)$ in region II is expanded in terms of an orthogonal and complete set of functions $\psi_{\mu\nu}(x, y)$

$$p(x, y) = \sum_{\mu=0}^{N_x-1} \sum_{\nu=0}^{N_y-1} a_{\mu\nu} \psi_{\mu\nu}(x, y) = \boldsymbol{\psi}^T \mathbf{a}, \quad (4)$$

where the sums have been truncated by N_x and N_y , “ T ” refers to transpose. $\boldsymbol{\psi}$ is a column vector, its elements are arranged as $(\mu, \nu) = (0, 0), (0, 1), \dots, (0, N_y -$

$1), (1, 0), (1, 1), \dots, (1, N_y - 1), \dots, (N_x - 1, 0), (N_x - 1, 1), \dots, (N_x - 1, N_y - 1)$.

We choose $\psi_{\mu,\nu}$ to be the eigenfunctions of closed *rigid* cavity defined by

$$\nabla^2 \psi_{\mu\nu} = -\gamma_{\mu\nu}^2 \psi_{\mu\nu}, \quad (5)$$

$$\left. \frac{\partial \psi_{\mu\nu}}{\partial x} \right|_{x=0 \text{ and } a/h} = 0, \quad \left. \frac{\partial \psi_{\mu\nu}}{\partial y} \right|_{y=0 \text{ and } 1} = 0. \quad (6)$$

By solving the eigenproblem of Eqs. (5) and (6), the eigenfunctions $\psi_{\mu\nu}$ and eigenvalues $\gamma_{\mu\nu}$ are given as $\psi_{\mu\nu} = (1/\sqrt{\Lambda_x \Lambda_y}) \cos(\mu\pi x/(a/h)) \cos(\nu\pi y)$ and $\gamma_{\mu\nu} = \sqrt{(\mu\pi)^2/(a/h)^2 + (\nu\pi)^2}$, respectively, where Λ_x and Λ_y are normalization coefficients.

Multiplying Eq. (1) by $\boldsymbol{\psi}$, integrating over x and y , applying Green's theorem, and using Eq. (5) and the boundary conditions Eq. (6), we obtain

$$p(x, y) = \int_0^1 \left[R(x, y, 0, y') \frac{\partial p(x', y')}{\partial x'} \Big|_{x'=0} - R(x, y, a, y') \frac{\partial p(x', y')}{\partial x'} \Big|_{x'=a/h} \right] dy', \quad (7)$$

(see Appendix), where

$$R(x, y, x', y') = \boldsymbol{\psi}^T(x, y) [K^2 \mathbf{I} - \mathbf{H}_{\text{in}}]^{-1} \boldsymbol{\psi}(x', y'). \quad (8)$$

In Eq. (8), \mathbf{I} refers to identity matrix, $\mathbf{H}_{\text{in}} = \boldsymbol{\Gamma} - \mathbf{j}KY\mathbf{C}^{\text{in}}$, where $\boldsymbol{\Gamma}$ is a diagonal matrix with elements $\gamma_{\mu\nu}^2$, and \mathbf{C}^{in} is a block diagonal matrix, its elements can be calculated analytically by

$$C_{\mu\nu, \mu'\nu'}^{\text{in}} = \int_0^{a/h} \psi_{\mu\nu}(x', 0) \psi_{\mu'\nu'}(x', 0) dx'. \quad (9)$$

With the help of Eq. (25), it can be noted that the eigenfunctions of the matrix \mathbf{H}_{in} are the modes of the closed cavity with the admittance on the bottom wall.

Equation (7) links the sound pressures in the scattering region (II) with their first derivatives with respect to x at the interfaces between the scattering region and the other two regions (I and III).

The sound pressure is written as a sum of the incident (amplitudes c_m) and reflected modes for region I, and only transmitted modes for region III

$$p(x, y) = \begin{cases} \sum_{m=0}^{M-1} c_m e^{jK_m^x x} \phi_m(y) + \sum_{m=0}^{M-1} \sum_{m'=0}^{M-1} R_{m,m'} c_m e^{-jK_{m'}^x x} \phi_{m'}(y), & x \leq 0, \\ \sum_{m=0}^{M-1} \sum_{m'=0}^{M-1} T_{m,m'} c_m e^{jK_{m'}^x (x-a/h)} \phi_{m'}(y), & x \geq a/h, \end{cases} \quad (10)$$

where $R_{m,m'}$ and $T_{m,m'}$ refer to the reflection and transmission coefficients, and M is the truncation number. $K_m^x = \sqrt{K^2 - \alpha_m^2}$ are axial wavenumbers of mode m in the rigid ducts. α_m and ϕ_m are the eigenvalues and eigenfunctions of transverse modes in regions I and III, they are given as $\alpha_m = m\pi$ and $\phi_m = \Lambda \cos(\alpha_m y)$, with Λ the normalization coefficients. Equation (10) is written in matrix form as

$$p(x, y) = \begin{cases} \boldsymbol{\phi}^T \mathbf{E}_0^+ \mathbf{c} + \boldsymbol{\phi}^T \mathbf{E}_0^- \mathbf{R} \mathbf{c}, & x \leq 0, \\ \boldsymbol{\phi}^T \mathbf{E}_a^+ \mathbf{T} \mathbf{c}, & x \geq a/h, \end{cases} \quad (11)$$

where \mathbf{E}_0^+ , \mathbf{E}_0^- , and \mathbf{E}_a^+ are $(M \times M)$ diagonal matrices with the elements $e^{jK_m^x x}$, $e^{-jK_m^x x}$, and $e^{jK_m^x (x-a/h)}$, respectively. $\boldsymbol{\phi}$ is a $(M \times 1)$ column vector, its elements are the eigenfunctions ϕ_m .

Substituting Eq. (11) into Eq. (7) at $x = 0$ and $x = a/h$, we obtain

$$\mathbf{I}_M + \mathbf{R} = j\mathbf{C}_0^T (K^2 \mathbf{I} - \mathbf{H}_{\text{in}})^{-1} (\mathbf{C}_0 \mathbf{K}^x (\mathbf{I}_M - \mathbf{R}) - \mathbf{C}_a \mathbf{K}^x \mathbf{T}), \quad (12)$$

$$\mathbf{T} = j\mathbf{C}_a^T (K^2 \mathbf{I} - \mathbf{H}_{\text{in}})^{-1} (\mathbf{C}_0 \mathbf{K}^x (\mathbf{I}_M - \mathbf{R}) - \mathbf{C}_a \mathbf{K}^x \mathbf{T}), \quad (13)$$

where \mathbf{K}^\times is a $(M \times M)$ diagonal matrix with elements K_m^x , and \mathbf{I}_M is a $(M \times M)$ identity matrix. The elements of matrices \mathbf{C}_0 and \mathbf{C}_a are

$$C_{0(a),\mu\nu,m} = \int_0^1 \psi_{\mu\nu}(x' = 0(a/h), y') \phi_m(y') dy', \quad (14)$$

where \mathbf{C}_0 and \mathbf{C}_a have dimensions $N \times M$ with $N = N_x \cdot N_y$. From Eqs. (12) and (13), we obtain

$$\begin{bmatrix} \mathbf{R} \\ \mathbf{T} \end{bmatrix} = [\mathbf{I}_{2M} + \mathbf{jGK}_{2M}^\times]^{-1} \{ -[\mathbf{I}_M, \mathbf{0}_M]^T + \mathbf{jC}_{0a}^T [K^2 \mathbf{I} - \mathbf{H}_{in}]^{-1} \mathbf{C}_0 \mathbf{K}^\times \}, \quad (15)$$

where $\mathbf{G} = \mathbf{C}_{0a}^T (K^2 \mathbf{I} - \mathbf{H}_{in})^{-1} \mathbf{C}_{0a}$, $\mathbf{C}_{0a} = [\mathbf{C}_0, \mathbf{C}_a]$ is a $(N \times 2M)$ matrix, \mathbf{I}_{2M} is a $(2M \times 2M)$ identity matrix, \mathbf{K}_{2M}^\times is a $(2M \times 2M)$ block diagonal matrix with two $(M \times M)$ diagonal matrices \mathbf{K}^\times on its main diagonal, and $\mathbf{0}_M$ is a $(M \times M)$ zero matrix.

If we assume that the problem is symmetric, the scattering matrix can be written as

$$\mathbf{S} = \begin{bmatrix} \mathbf{R} & \mathbf{T} \\ \mathbf{T} & \mathbf{R} \end{bmatrix} = [\mathbf{I}_{2M} + \mathbf{jGK}_{2M}^\times]^{-1} [-\mathbf{I}_{2M} + \mathbf{jGK}_{2M}^\times]. \quad (16)$$

The scattering matrix \mathbf{S} can be expressed as²⁴

$$\mathbf{S} = -\mathbf{I}_{2M} + 2\mathbf{jC}_{0a}^T [K^2 \mathbf{I} - \mathbf{H}_{eff}]^{-1} \mathbf{C}_{0a} \mathbf{K}_{2M}^\times, \quad (17)$$

(see Appendix), where

$$\mathbf{H}_{eff} = \mathbf{H}_{in} - \mathbf{jC}_{0a} \mathbf{K}_{2M}^\times \mathbf{C}_{0a}^T. \quad (18)$$

The eigenvalues K_λ and eigenfunctions $\tilde{\varphi}_\lambda = \boldsymbol{\psi}^T \mathbf{V}_\lambda$ are defined by the eigenproblem of matrix \mathbf{H}_{eff} ,

$$\mathbf{H}_{eff} \mathbf{V}_\lambda = K_\lambda^2 \mathbf{V}_\lambda. \quad (19)$$

They describe the complex resonances of scattering region II, which is opened to infinities through regions I and III, and truncated at the interfaces, $x = 0$ and $x = a/h$. The elements of vector $\boldsymbol{\psi}$ are the eigenfunctions of the *rigid* closed cavity defined by Eqs. (5) and (6). Because the eigenfunctions $\tilde{\varphi}_\lambda$ in scattering region II are non-separable in x and y , we use only one index λ to describe the eigenvalues K_λ and the eigenfunctions $\tilde{\varphi}_\lambda$. It is noted that the complex resonances are calculated in Refs. 20 and 13 by finite element method with absorbing boundary conditions.

With the help of eigenvectors \mathbf{V}_λ , Eq. (17) can be written as

$$\begin{aligned} \mathbf{S} &= -\mathbf{I}_{2M} + 2j\mathbf{C}_{0a}^T \mathbf{V} [K^2 \mathbf{V} \mathbf{V}^{-1} - \mathbf{V} \mathbf{H}_{\text{eff}} \mathbf{V}^{-1}]^{-1} \mathbf{V}^T \mathbf{C}_{0a} \mathbf{K}_{2M}^\times \\ &= -\mathbf{I}_{2M} + 2j\tilde{\mathbf{C}}_{0a}^T [K^2 \mathbf{I} - \mathbf{K}_\lambda]^{-1} \tilde{\mathbf{C}}_{0a} \mathbf{K}_{2M}^\times, \end{aligned} \quad (20)$$

where \mathbf{K}_λ is a $(N \times N)$ diagonal matrix with K_λ^2 its main elements. \mathbf{V} is a $(N \times N)$ matrix with its columns the eigenvectors \mathbf{V}_λ of matrix \mathbf{H}_{eff} . \mathbf{H}_{eff} is a symmetric non-Hermitian matrix, its eigenvectors are bi-orthogonal. Hence, $\mathbf{V}^{-1} = \mathbf{V}^T$ has been used in Eq. (20). Matrix $\tilde{\mathbf{C}}_{0a}$ is defined as

$$\begin{aligned} \tilde{\mathbf{C}}_{0a} = \mathbf{V}^T \mathbf{C}_{0a} &= \int_0^h \mathbf{V}^T [\boldsymbol{\psi}(x' = 0, y') \boldsymbol{\phi}^T(y'), \boldsymbol{\psi}(x' = a/h, y') \boldsymbol{\phi}^T(y')] dy' \\ &= \int_0^h [\tilde{\boldsymbol{\varphi}}(x' = 0, y') \boldsymbol{\phi}^T(y'), \tilde{\boldsymbol{\varphi}}(x' = a/h, y') \boldsymbol{\phi}^T(y')] dy', \end{aligned} \quad (21)$$

where $\tilde{\boldsymbol{\varphi}}(x' = 0, y')$ and $\tilde{\boldsymbol{\varphi}}(x' = a/h, y')$ are $(N \times 1)$ vectors with elements the eigenfunctions $\tilde{\varphi}_\lambda$ of scattering region II at $x' = 0$ and $x' = a/h$, respectively. Matrix $\tilde{\mathbf{C}}_{0a}$ describes the couplings of the scattering region II with regions I and III. Equation (20) is not valid at exceptional points at which the eigenvalues and eigenfunctions coalesce, and therefore \mathbf{V}^{-1} is singular.

Equation (20) extends the traditional acoustic resonance scattering formula²¹, in which the complex eigenfrequencies of scattering region give the resonance poles, to describe the coupling effects between scattering region and rigid waveguides.

III. RESULTS AND DISCUSSIONS

First, we show how the trapped modes with real resonance frequencies occur in the vicinity of exceptional points and how they are linked to avoided crossings of the eigenvalues of matrix \mathbf{H}_{eff} . Second, we show that a transmission zero is present in the vicinity of a resonance peak when the real resonance frequency is crossed. Finally, we consider the effects of dissipation in acoustic absorbing material. The liner can be described by an impedance model ($Y = 1/Z$):

$$Z = Re + j \cot(Kd_l/h), \quad (22)$$

where d_l/h is the normalized depth of the liner, and Re is the resistance. Z is assumed to be uniform. All the numerical results are calculated with the truncation number $M = 30$, $N_x = 30$, and $N_y = 30$. Although Eqs. (17) and (20) are valid for arbitrary multimodal incidences, for the sake of simplicity, we assume that only plane waves are incident in the following.

The eigenvalues of matrix \mathbf{H}_{in} , denoted $\beta_{\mu,\nu}^2$, represent the eigenvalues of the closed cavity with the admittance. The trajectories of $\Re(\beta_{\mu,\nu})$ as a function of $|KY|$ are shown in Fig. 2 with $a/h = 4$ and $Re = 0$. When the eigenvalue curves cross, the modes are degenerate²⁵. At the degeneracies,

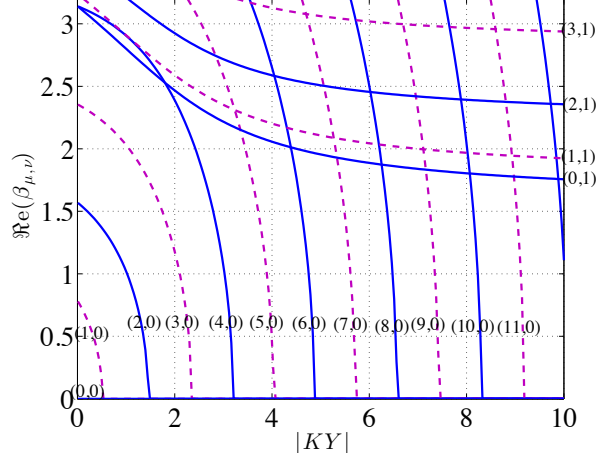


Figure 2: (Color online) Trajectories of the real parts of eigenvalues $\beta_{\mu,\nu}$ of the closed cavity with admittance as a function of $|KY|$ with $Re = 0$ and $a/h = 4$. Solid lines label even modes in x -direction, dashed lines label odd modes in x -direction. The mode indices (μ, ν) are marked near each curve.

eigenvalues coalesce, while eigenfunctions are still bi-orthogonal²⁵ and there is no interaction between the modes.

We consider the modes behaviour when the region II is opened. It can be modelled by matrix \mathbf{H}_{eff} which depends on three parameters: a/h , KY , and K . This is due to the K dependences of both the impedance boundary condition KY and the effective radiation condition at the interfaces $x = 0$ and $x = a/h$ (the term \mathbf{K}_{2M}^x in Eq. (18)). In Fig. 3, we plot the eigenvalue trajectories as a function of $|KY|$ with $a/h = 4$ and $K = 2.5$. The curves with the same symmetry about x , which had crossings before in Fig. 2, now have avoided crossings in Fig. 3. The avoided crossings of the eigenvalues

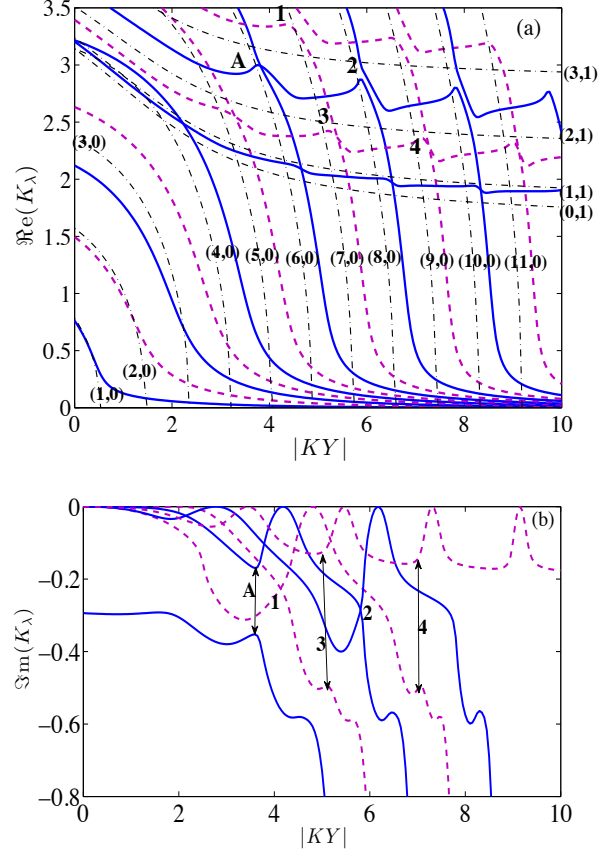


Figure 3: (Color online) Trajectories of $\Re(K_\lambda)$ and $\Im(K_\lambda)$ of matrix \mathbf{H}_{eff} as a function of $|KY|$ with $K = 2.5$, $a/h = 4$, and $Re = 0$: (a) real parts and (b) imaginary parts. Solid lines and dashed lines correspond to different symmetries as shown in Fig. 2. For comparison, we plot also the trajectories of $\Re(\beta_{\mu,\nu})$ of the closed cavity by dash-dot lines.

K_λ in Fig. 3 occur in the vicinity of the degeneracies of the closed cavity, for example those labelled by A, 1, 2, 3, and 4, respectively. Avoided crossings, already known in structural dynamics^{26,27,28}, are less used in cavities lined

with impedance.

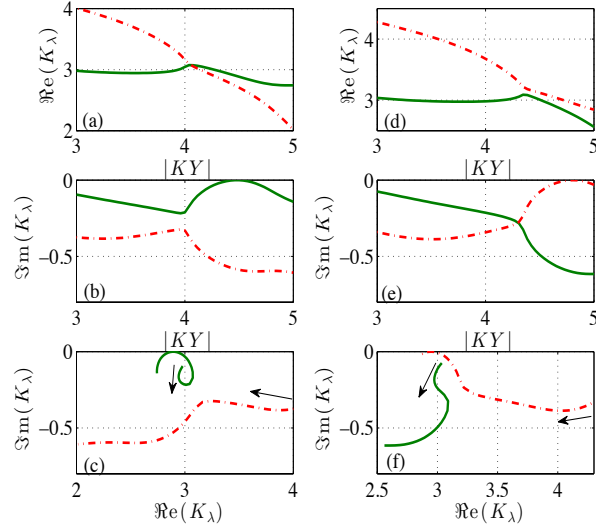


Figure 4: (Color online) Two types of avoided crossings of K_λ as a function $|KY|$ with $K = 2.5$ under different values of a/h : (a), (b) and (c) for $a/h = 3.8$; (d), (e) and (f) for $a/h = 3.6$. They have the same two modes as avoided crossing “A” in Fig. 3. EP occurs at $|KY| = 4.18$ and $a/h = 3.7$, labelled by “C₁” in Fig. 5. At (b) $|KY| = 4.5$ and (e) $|KY| = 4.8$, $\Im m(K_\lambda)$ goes to zero. K_λ turns to be a real resonance frequency.

As we mentioned before, the matrix \mathbf{H}_{eff} depends on three parameters. Another parameter, the liner length a/h , is used here to manipulate the avoided crossing. Taking the same two modes with avoided crossing “A” in Fig. 3 as an example, we decrease the liner length a/h , the results are shown in Fig. 4. When a/h varies, there is a jump between two types of avoided crossings. When $a/h = 3.8$, there is a crossing for $\Re(K_\lambda)$ and not

for $\Im m(K_\lambda)$ (see Fig. 4 (a) and (b)), while for $a/h = 3.6$, there is no crossing for $\Re e(K_\lambda)$ and crossing for $\Im m(K_\lambda)$ (see Fig. 4 (d) and (e)).

These findings and the type change of the avoided crossings from Fig. 4 (c) to (f) suggest that there should exist a critical value a_{cri}/h , with which the curves of K_λ as a function of $|KY|$ will cross at a critical value $|KY|_{cri}$. We found that at $|KY| = 4.18$, $a/h = 3.7$, and $K = 2.5$, the two eigenvalues coalesce, so do their eigenfunctions. $(a_{cri}/h, |KY|_{cri})$ is called an Exceptional Point (EP) in the parameter plane $(a/h, |KY|)$. A strong mixing of the eigenfunctions of the two modes occurs near the EP. The two modes which participate in the avoided crossing exchange their identities^{26,27}.

Avoided crossing occurs in the vicinity of an EP. EPs were first introduced by Kato²⁹, and were extensively developed by Heiss^{30,31,32}, Rotter^{33,34,35}, and Berry³⁶. The mathematically topological structures of Riemann sheets at an EP, depend on a complex or two real parameters. A typical EP distribution of H_{eff} in the plane of $|KY|$ and a/h , with K fixed, is shown in Fig. 5. They occur near the crossings between two modes in the closed cavity that have the same symmetry about x . The branches A and C (B and D) correspond to the crossings between two modes in the closed cavity with even (odd) symmetry about x .

It is remarkable that at $|KY| = 4.5$ in Fig. 4 (b) and $|KY| = 4.8$ in Fig. 4 (e), $\Im m(K_\lambda)$ goes to zero. This is a real resonance frequency in the *open* scattering region II. It is this kind of mode that Friedrich *et al*¹⁸ found in nuclear reaction, and Sadreev *et al*.¹⁹ found in quantum billiards. This is

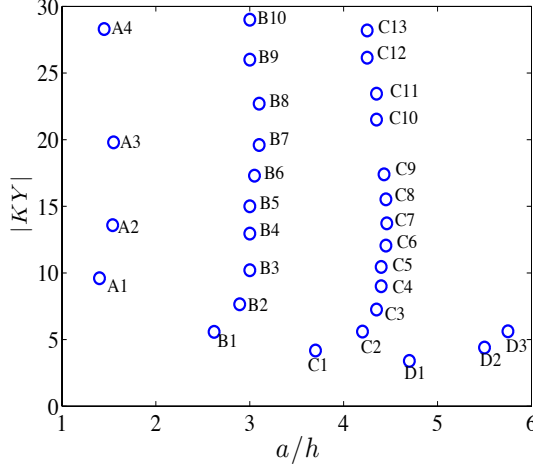


Figure 5: (Color online) The distribution of EPs of \mathbf{H}_{eff} in the $(a/h, |KY|)$ plane with $K = 2.5$. The branches A and C (B and D) correspond to the crossings between two modes in closed cavity with even (odd) symmetry about x .

the trapped mode that plays a crucial role in a transmission zero in the lined waveguide.

To realize a practical design of transmission zero, we need to understand the modes behaviour in the parameters space $(a/h, d_l/h, K)$. We re-produce Fig. 4 in Fig. 6 using d_l/h as a varying parameter. It is quite surprising that the eigenvalue trajectories in the two different parameter spaces of Figs. 4 and 6 are very similar to each other. We find that at $a/h = 3.8$ and $d_l/h = 0.425$, real resonance (trapped mode) occurs, with $K = 2.5$.

As pointed out earlier, \mathbf{H}_{eff} depends on frequency K , so do K_λ . To find the frequency at which transmission zero occurs, we need to solve equation

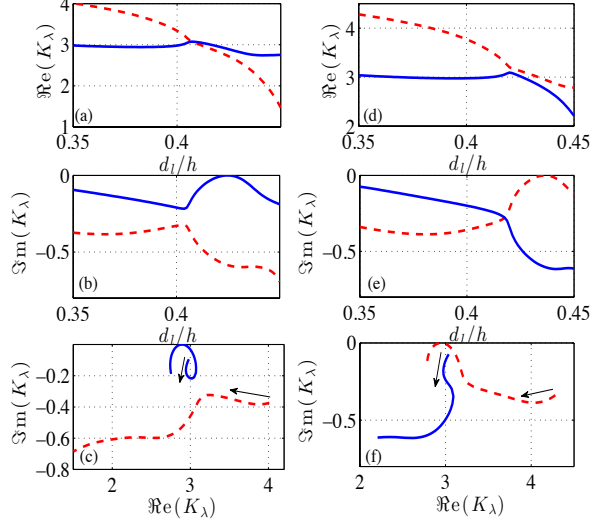


Figure 6: (Color online) Re-plot Fig. 4 using d_l/h , the liner depth, as x-coordinate.

$K = K_\lambda(K)$. Therefore, near the EP labelled by “ C_1 ” in Fig. 5, the real resonance frequency we seek for corresponds to the point where the curves $y = K_\lambda(K, d_l/h, a/h = 3.8)$ cross the line $y = K$. We find that at $K = 2.853$, $d_l/h = 0.35$, and $a/h = 3.8$, real resonance (trapped mode) occurs. Using this group of parameters, we calculate the transmission and reflection coefficients of the plane mode by Eq. (16), as shown in Fig. 7. A transmission zero occurs at $K = 2.853$. The corresponding sound pressure field is shown in Fig. 8. At the same time, reflection coefficient has a peak with amplitude 1.

Now we consider the effects of dissipation. A small Re is added in the impedance model Eq. (22). In Fig. 9, we plot the reflection and transmission coefficients as a function of K with $d_l/h = 0.35$ and $a/h = 3.8$ under

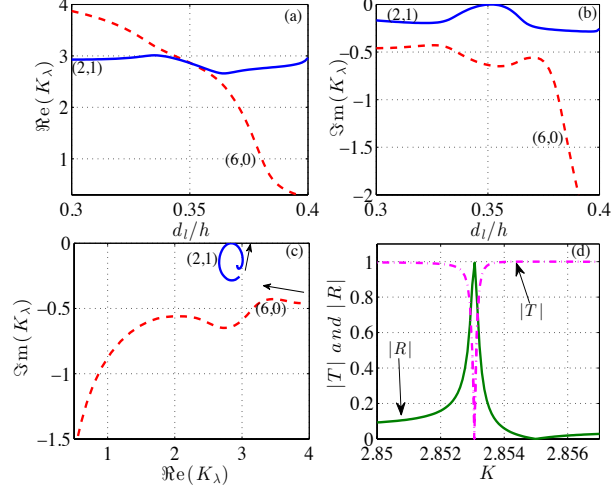


Figure 7: (Color online) Transmission and reflection coefficients of the plane mode and trajectories of eigenvalues K_λ of matrix \mathbf{H}_{eff} as a function of d_l/h with $K = 2.85$, $a/h = 3.8$, and $Re = 0$: (a) real parts, (b) imaginary parts, (c) in complex K_λ plane, and (d) transmission and reflection coefficients as a function of K with $d_l/h = 0.35$, $a/h = 3.8$, and $Re = 0$. In the figure, we also label the indices of the corresponding mode in closed cavity.

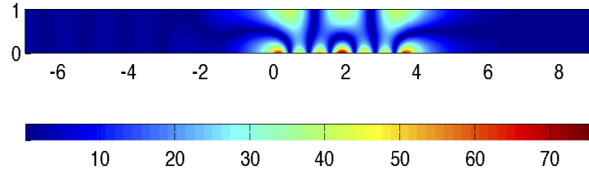


Figure 8: (Color online) The absolute value of sound pressure field in the waveguide when real resonance frequency is crossed.

different values of Re . The amplitude peaks of the reflection and transmission coefficients decrease rapidly with increasing Re . The high sensitivity on the dissipation is due to the fact that the crucial ingredient to form Fano resonance in the transmission and reflection coefficients – the trapped mode

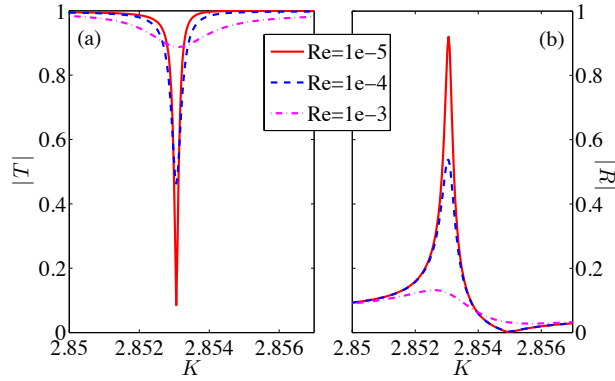


Figure 9: (Color online) (a) Transmission and (b) reflection coefficients of the plane mode as a function of frequency under different values of resistance Re with $d_l/h = 0.35$.

with real resonance frequency, turns to be quasi-trapped mode with complex resonance frequency. The sharp asymmetric profile becomes smoother, as shown in Fig. 9.

IV. CONCLUSIONS

We have shown that the acoustic scattering matrix can be efficiently described with the help of an effective matrix \mathbf{H}_{eff} . This effective matrix

is linked to the resonances of the scattering region opened to the infinite waveguides and gives the poles of the scattering matrix. Those poles are in the vicinity of exceptional points.

There are an infinite number of exceptional points in the parameters plane $(a/h, |KY|)$, at which the eigenvalues and eigenfunctions of two modes coalesce, for the *open* lined section. In the vicinity of each exceptional point, crossing or avoided crossing of the real and imaginary parts of the complex resonances (eigenvalues) occur. By varying one of the parameters, say $|KY|$, one mode turns to be a trapped mode, its resonance frequency becomes real. When a plane mode is incident, a transmission zero is present in the vicinity of a resonance peak, called Fano resonance, in the transmission amplitudes when the real resonance frequency is crossed.

EPs, real resonance frequencies, and transmission zeros can also be obtained for parameters $(a/h, d_l/h)$, which can suit the practical need of noise mitigation. We have also shown that the transmission zeros and peaks are highly sensitive to the dissipation.

With the aid of the eigenvalues and eigenfunctions of matrix \mathbf{H}_{eff} , the traditional acoustic resonance scattering formula is extended to describe the coupling effects between the open lined section and the rigid parts of the waveguide.

In this paper, the numerical calculations are made for one incident mode and thus “zero transmission” means that the total sound field is stopped. However, the model is valid for multimode being incident. To stop the total

sound field for multimode propagation is still an open question.

Acknowledgements

We gratefully acknowledge the support from the European Union through ITN-project FlowAirS (Contract No. FP7-PEOPLE-2011-ITN-289352).

Appendix: Derivation of Eq. (7) and (17)

1. Derivation of Eq. (7)

Multiplying Eq. (1) by ψ , integrating over the closed cavity, we obtain

$$\int_0^1 \int_0^{a/h} \psi \left(\frac{\partial^2 p}{\partial x^2} + \frac{\partial^2 p}{\partial y^2} \right) dx dy = -K^2 \int_0^1 \int_0^{a/h} \psi p dx dy. \quad (23)$$

Applying Green's theorem for Eq. (23), substituting Eq. (5) into the resulting equation, we have

$$\begin{aligned} & \int_0^1 \left(\psi \frac{\partial p}{\partial x} - \frac{\partial \psi}{\partial x} p \right) \Big|_{x=0}^{x=a/h} dy + \int_0^{a/h} \left(\psi \frac{\partial p}{\partial y} - \frac{\partial \psi}{\partial y} p \right) \Big|_{y=0}^{y=1} dx \\ &= -(K^2 \mathbf{l} - \Gamma) \int_0^1 \int_0^{a/h} \psi p dx dy, \end{aligned} \quad (24)$$

where \mathbf{l} is an identity matrix, and Γ is a diagonal matrix with elements $\gamma_{\mu\nu}^2$.

Substituting the boundary conditions, Eqs. (3) and (6), into Eq. (24), results in

$$\int_0^1 \left(\psi \frac{\partial p}{\partial x} \right) \Big|_{x=a/h}^{x=0} dy - jKY \int_0^{a/h} \psi(x, 0) p(x, 0) dx = (K^2 \mathbf{l} - \Gamma) \int_0^1 \int_0^{a/h} \psi p dx dy. \quad (25)$$

Replacing the pressure function p inside the scattering region by Eq. (4), and using the orthogonality property of eigenfunctions $\psi_{\mu\nu}$, the expansion

coefficients \mathbf{a} can be written as

$$\mathbf{a} = \left[K^2 \mathbf{I} - \Gamma + jKY \int_0^{a/h} \boldsymbol{\psi}(x, 0) \boldsymbol{\psi}^T(x, 0) dx \right]^{-1} \int_0^1 \left(\boldsymbol{\psi} \frac{\partial p}{\partial x} \right) \Big|_{x=a/h}^{x=0} dy. \quad (26)$$

Substitute the upper expression of \mathbf{a} into Eq. (4), we end up with Eq. (7).

2. Derivation of Eq. (17)

Due to the symmetry property of the matrix \mathbf{S} , Eq. (16) can be rewritten as

$$\mathbf{S} = -\mathbf{I}_{2M} + \frac{2j\mathbf{C}_{0a}^T (K^2 \mathbf{I} - \mathbf{H}_{in})^{-1} \mathbf{C}_{0a} \mathbf{K}_{2M}^x}{\mathbf{I}_{2M} + j\mathbf{C}_{0a}^T (K^2 \mathbf{I} - \mathbf{H}_{in})^{-1} \mathbf{C}_{0a} \mathbf{K}_{2M}^x}. \quad (27)$$

Now we expand the denominator in Eq. (27) into a geometric series²⁴,

$$\begin{aligned} \mathbf{S} &= -\mathbf{I}_{2M} + 2j\mathbf{C}_{0a}^T \frac{1}{K^2 \mathbf{I} - \mathbf{H}_{in}} \mathbf{C}_{0a} \mathbf{K}_{2M}^x \sum_{q=0}^{\infty} \left(-j\mathbf{C}_{0a}^T \frac{1}{K^2 \mathbf{I} - \mathbf{H}_{in}} \mathbf{C}_{0a} \mathbf{K}_{2M}^x \right)^q \\ &= -\mathbf{I}_{2M} + 2j\mathbf{C}_{0a}^T \frac{1}{K^2 \mathbf{I} - \mathbf{H}_{in}} \sum_{q=0}^{\infty} \left(-j\mathbf{C}_{0a} \mathbf{K}_{2M}^x \mathbf{C}_{0a}^T \frac{1}{K^2 \mathbf{I} - \mathbf{H}_{in}} \right)^q \mathbf{C}_{0a} \mathbf{K}_{2M}^x \\ &= -\mathbf{I}_{2M} + 2j\mathbf{C}_{0a}^T \frac{1}{K^2 \mathbf{I} - \mathbf{H}_{in}} \frac{1}{1 + j\mathbf{C}_{0a} \mathbf{K}_{2M}^x \mathbf{C}_{0a}^T \frac{1}{K^2 \mathbf{I} - \mathbf{H}_{in}}} \mathbf{C}_{0a} \mathbf{K}_{2M}^x \\ &= -\mathbf{I}_{2M} + 2j\mathbf{C}_{0a}^T \frac{1}{K^2 \mathbf{I} - \mathbf{H}_{in} + j\mathbf{C}_{0a} \mathbf{K}_{2M}^x \mathbf{C}_{0a}^T} \mathbf{C}_{0a} \mathbf{K}_{2M}^x. \end{aligned} \quad (28)$$

By the expression of \mathbf{K}_N , the upper equation results in the Eq. (17).

REFERENCES

- ¹ B. Beck, N. Schiller, and M. Jones, “Impedance assessment of an acoustic metamaterial-inspired acoustic liner”, J. Acoust. Soc. Am. **134**, 4222–4222 (2013).

- ² J.-P. Groby, W. Huang, A. Lardeau, and Y. Aurégan, “The use of slow waves to design simple sound absorbing materials”, *J. Appl. Phys.* **117**, 124903 (2015).
- ³ D. L. Lansing and W. E. Zorumski, “Effects of wall admittance changes on duct transmission and radiation of sound”, *J. Sound Vib.* **27**, 85–100 (1973).
- ⁴ J. F. Unruh, “Finite length tuning for low frequency lining design”, *J. Sound Vib.* **45**, 5–14 (1976).
- ⁵ W. Koch, “Attenuation of sound in multi-element acoustically lined rectangular ducts in the absence of mean flow”, *J. Sound Vib.* **52**, 459–496 (1977).
- ⁶ C. R. Fuller, “Propagation and radiation of sound from flanged circular ducts with circumferentially varying wall admittances, I: Semi-infinite ducts”, *J. Sound Vib.* **93**, 321–340 (1984).
- ⁷ W. R. Watson, M. G. Jones, T. L. Parrott, and J. Sobieski, “Assessment of Equation Solvers and Optimization Techniques for Nonaxisymmetric Liners”, *AIAA Journal* **42**, 2010–2018 (2004).
- ⁸ B. Regan and J. Eaton, “Modeling the influence of acoustic liner non-uniformities on duct modes”, *J. Sound Vib.* **219**, 859–879 (1999).
- ⁹ W. Bi, V. Pagneux, D. Lafarge, and Y. Aurégan, “Modelling of sound

- propagation in a non-uniform lined duct using a multi-modal propagation method”, *J. Sound Vib.* **289**, 1091–1111 (2006).
- ¹⁰ B. Luk’yanchuk, N. I. Zheludev, S. A. Maier, N. J. Halas, P. Nordlander, H. Giessen, and C. T. Chong, “The fano resonance in plasmonic nanostructures and metamaterials”, *Nature Mater.* **9**, 707–715 (2010).
 - ¹¹ A. E. Miroshnichenko, S. Flach, and Y. S. Kivshar, “Fano resonances in nanoscale structures”, *Rev. Mod. Phys.* **82**, 2257–2298 (2010).
 - ¹² U. Fano, “Effects of configuration interaction on intensities and phase shifts”, *Phys. Rev.* **124**, 1866–1878 (1961).
 - ¹³ S. Hein, W. Koch, and L. Nannen, “Trapped modes and fano resonances in two-dimensional acoustical duct-cavity systems”, *J. Fluid Mech.* **692**, 257–287 (2012).
 - ¹⁴ R. Parker, “Resonance effects in wake shedding from parallel plates: Some experimental observations”, *J. Sound Vib.* **4**, 62–72 (1966).
 - ¹⁵ Y. Duan, W. Koch, C. M. Linton, and M. McIVER, “Complex resonances and trapped modes in ducted domains”, *J. Fluid Mech.* **571**, 119–147 (2007).
 - ¹⁶ V. Pagneux, “Trapped modes and edge resonances in acoustics and elasticity”, *CISM International Centre for Mechanical Sciences* **547**, 181–223 (2013).

- ¹⁷ von Neumann and E. P. Wigner, “Über merkwürdige diskrete eigenwerte”, Phys. Z **30**, 465–467 (1929).
- ¹⁸ H. Friedrich and D. Wintgen, “Interfering resonances and bound states in the continuum”, Phys. Rev. A **32**, 3231–3242 (1985).
- ¹⁹ A. Sadreev, E. Bulgakov, and I. Rotter, “Bound states in the continuum in open quantum billiards with a variable shape”, Phys. Rev. B **73**, 235342 (2006).
- ²⁰ S. Hein, W. Koch, and L. Nannen, “Fano resonances in acoustics”, J. Fluid Mech. **664**, 238–264 (2010).
- ²¹ L. Flax, G. Gaunaurd, and H. Uberall, *Theory of Resonance scattering, in Physical Acoustics: Principles and Methods, Vol. XV, Eds., W. P. Mason and R. N. Thurston* (Academic Press) (1999), Chap. 3, pp. 191–294.
- ²² P. Racec, E. Racec, and H. Neidhardt, “Evanescent channels and scattering in cylindrical nanowire heterostructures”, Phys. Rev. B **79**, 155305 (2009).
- ²³ E. R. Racec, U. Wulf, and P. N. Racec, “Fano regime of transport through open quantum dots”, Phys. Rev. B **82**, 085313 (2010).
- ²⁴ H.-J. Stöckmann, E. Persson, Y.-H. Kim, M. Barth, U. Kuhl, and I. Rotter, “Effective hamiltonian for a microwave billiard with attached waveguide”, Phys. Rev. E **65**, 066211 (2002).

- ²⁵ P. M. Morse and K. U. Ingard, *Theoretical acoustics* (McGraw-Hill Book Company, New York) (1968), Chap. 5, pp. 206.
- ²⁶ A. W. Leissa, “On a curve veering aberration”, J. Applied Math. and Phys. (ZAMP) **25**, 99–111 (1974).
- ²⁷ J. R. Kuttler and V. G. Sigillito, “On curve veering”, J. Sound and Vib. **75**, 585–588 (1981).
- ²⁸ N. C. Perkins and C. D. Mote, “Comments on curve veering in eigenvalue problems”, J. Sound and Vib. **106**, 451–463 (1986).
- ²⁹ T. Kato, *Perturbation Theory of Linear Operators* (Berlin: Springer) (1966), pp. 64.
- ³⁰ W. D. Heiss and A. L. Sannino, “Avoided level crossing and exceptional points”, J. Phys. A: Math. Gen. **23**, 1167–1178 (1990).
- ³¹ W. D. Heiss, “Repulsion of resonance states and exceptional points”, Phys. Rev. E **61**, 929–932 (2000).
- ³² W. D. Heiss, “Exceptional points of non-hermitian operators”, J. Phys. A: Math. Gen. **37**, 2455–2464 (2004).
- ³³ I. Rotter, “A non-hermitian hamilton operator and the physics of open quantum systems”, J. Phys. A: Math.Theor. **42**, 153001 (2009).
- ³⁴ U. Gunther, I. Rotter, and B. Samsonov, “Projective hilbert space structures at exceptional points”, J. Phys. A: Math. Theor. **40**, 8815–8833 (2007).

- ³⁵ M. Muller and I. Rotter, “Exceptional points in open quantum systems”, J. Phys. A: Math. Theor. **41**, 244018 (2008).
- ³⁶ M. V. Berry, “Physics of nonhermitian degeneracies”, Czechoslovak J. of Phys. **54**, 1039–1047 (2004).

LIST OF FIGURES

- FIG. 1 (Color online) A two-dimensional infinite waveguide lined with a locally reacting material of length a . Y refers to the admittance. The closed counterpart of the scattering region is called *closed cavity*, with rigid conditions at $x = 0$ and $x = a$ 7
- FIG. 2 (Color online) Trajectories of the real parts of eigenvalues $\beta_{\mu,\nu}$ of the closed cavity with admittance as a function of $|KY|$ with $Re = 0$ and $a/h = 4$. Solid lines label even modes in x -direction, dashed lines label odd modes in x -direction. The mode indices (μ, ν) are marked near each curve. 13
- FIG. 3 (Color online) Trajectories of $\Re(K_\lambda)$ and $\Im(K_\lambda)$ of matrix \mathbf{H}_{eff} as a function of $|KY|$ with $K = 2.5$, $a/h = 4$, and $Re = 0$: (a) real parts and (b) imaginary parts. Solid lines and dashed lines correspond to different symmetries as shown in Fig. 2. For comparison, we plot also the trajectories of $\Re(\beta_{\mu,\nu})$ of the closed cavity by dash-dot lines. 14
- FIG. 4 (Color online) Two types of avoided crossings of K_λ as a function $|KY|$ with $K = 2.5$ under different values of a/h : (a), (b) and (c) for $a/h = 3.8$; (d), (e) and (f) for $a/h = 3.6$. They have the same two modes as avoided crossing “A” in Fig. 3. EP occurs at $|KY| = 4.18$ and $a/h = 3.7$, labelled by “ C_1 ” in Fig. 5. At (b) $|KY| = 4.5$ and (e) $|KY| = 4.8$, $\Im(K_\lambda)$ goes to zero. K_λ turns to be a real resonance frequency. 15

FIG. 5 (Color online) The distribution of EPs of \mathbf{H}_{eff} in the $(a/h, KY)$ plane with $K = 2.5$. The branches A and C (B and D) correspond to the crossings between two modes in closed cavity with even (odd) symmetry about x	17
FIG. 6 (Color online) Re-plot Fig. 4 using d_l/h , the liner depth, as x-coordinate.	18
FIG. 7 (Color online) Transmission and reflection coefficients of the plane mode and trajectories of eigenvalues K_λ of matrix \mathbf{H}_{eff} as a function of d_l/h with $K = 2.85, a/h = 3.8$, and $Re = 0$: (a) real parts, (b) imaginary parts, (c) in complex K_λ plane, and (d) transmission and reflection coefficients as a function of K with $d_l/h = 0.35, a/h = 3.8$, and $Re = 0$. In the figure, we also label the indices of the corresponding mode in closed cavity.	19
FIG. 8 (Color online) The absolute value of sound pressure field in the waveguide when real resonance frequency is crossed.	19
FIG. 9 (Color online) (a) Transmission and (b) reflection coefficients of the plane mode as a function of frequency under different values of resistance Re with $d_l/h = 0.35$	20